Cathepsin B-sensitive polymers for compartment-specific degradation and nucleic acid release

David S.H. Chu[a], **Russell N. Johnson**[a], and **Suzie H. Pun**[a,*]

[a]Department of Bioengineering, University of Washington, Seattle, Washington, 98195

Abstract

Degradable cationic polymers are desirable for *in vivo* nucleic acid delivery because they offer significantly decreased toxicity over non-degradable counterparts. Peptide linkers provide chemical stability and high specificity for particular endopeptidases but have not been extensively studied for nucleic acid delivery applications. In this work, enzymatically degradable peptide-HPMA copolymers were synthesized by RAFT polymerization of HPMA with methacrylated peptide macromonomers, resulting in polymers with low polydispersity and near quantitative incorporation of peptides. Three peptide-HPMA copolymers were evaluated: (i) $pHCathK_{10}$, containing peptides composed of the linker phe-lys-phe-leu (FKFL), a substrate of the endosomal/lysosomal endopeptidase cathepsin B, connected to oligo-(L)-lysine for nucleic acid binding, (ii) $pHCath(D)K_{10}$, containing the FKFL linker with oligo-(D)-lysine, and (iii) $pH(D)Cath(D)K_{10}$, containing all (D) amino acids. Cathepsin B degraded copolymers $pHCathK_{10}$ and $pHCath(D)K_{10}$ within one hour while no degradation of $pH(D)Cath(D)K_{10}$ was observed. Polyplexes formed with $pHCathK_{10}$ copolymers show DNA release by 4 hrs of treatment with cathepsin B; comparatively, polyplexes formed with $pHCath(D)K_{10}$ and $pH(D)Cath(D)K_{10}$ show no DNA release within 8 hrs. Transfection efficiency in HeLa and NIH/3T3 cells were comparable between the copolymers but $pHCathK_{10}$ was less toxic. This work demonstrates the successful application of peptide linkers for degradable cationic polymers and DNA release.

Keywords

non-viral gene delivery; cathepsin B; RAFT polymerization

1. Introduction

Polycations are frequently used as nucleic acid delivery materials because of their ability to package nucleic acids and promote cellular uptake [1]. However, polycation toxicity is frequently a limiting factor for *in vivo* application, thus impeding clinical translation [2–4]. Both nucleic acid delivery efficiency and cytotoxicity have been correlated with increasing molecular weight for several polycations [5, 6]. Higher molecular weight polycations provide stronger binding to nucleic acids, resulting in improved stability in serum and circulation time after systemic delivery [7–9]. Lower molecular weight polycations are more readily displaced from their nucleic acid cargo; this release is necessary for biological

*Corresponding Author: spun@u.washington.edu 3720 15th Ave NE Foege N530P, Box 355061 Seattle, WA 98195 (206) 685 3488.

activity [10]. Lower MW materials are also less toxic to cells when compared to their higher molecular weight counterparts [11, 12]. Biodegradable polycations with controllable degradation have been of great interest to the nucleic acid delivery field because these materials can provide combine advantages of both high and low molecular weight polycations.

The most extensively studied degradable cationic polymers have utilized either reducible or hydrolysable bonds [13–16], but these approaches provide limited control over the *in vivo* site of degradation. For example, poly(beta-amino esters) are degraded more quickly at neutral pH than acidic pH so that delivery vehicles would be susceptible to degradation once reconstituted in aqueous solution and administered *in vivo* [16]. Reducible linkers aim to take advantage of the highly reducing cytosolic environment for controlled intracellular degradation [17], but extracellular reduction has been implicated as the primary site of degradation for some polymeric systems [18]. We recently synthesized reducible HPMA-*co*-oligolysine copolymers by including disulfide linkers between the HPMA backbone and oligolysine pendant peptides [19]. Although reduced cytotoxicity was observed with these materials, transfection efficiency was also significantly decreased. This was partially attributed to the instability of the disulfide bond by sulfhydryl exchange and metal-catalyzed oxidation of the free sulfhydryl groups leading to crosslinking between polymer strands.

A controlled release material with polymer degradation triggered by specific intracellular enzymatic activity is highly attractive for gene delivery applications. Enzyme-catalyzed degradation combines chemical stability and high specificity. Peptide-based linkers act as selective substrates for specific extra- or intracellular peptidases, with enzymatic specificity determined by the amino acid sequence. In addition, linkers have varying rates of enzymatic cleavage, adjustable by changing the recognition sequence or neighboring residues [20, 21], further enabling the control of degradation. Peptide linkers have been used successfully for other biological applications, such as antibody-drug conjugates for cancer therapy [22] and degradable cross-linked scaffolds for tissue engineering [23], but have not been extensively studied for nucleic acid delivery applications. Two groups recently reported enzymatically-cleavable linkers for release of targeting ligands [24, 25], but, to our knowledge, no reports using peptide linkers in main or side-chain architectures in gene delivery materials as an approach for specific polymer degradation are available.

In nucleic acid delivery applications, endosomal degradation of carriers has several advantages. Materials need to remain intact in the extracellular environment to protect nucleic acids from nucleases present in serum. However, polycations such as polyethylenimine (PEI) and poly-(L)-lysine (PLL) have been shown to trigger mitochondrial-mediated apoptosis after polymer interaction with the outer mitochondrial membrane [26]. Polymers that degrade prior to cytosolic release are therefore hypothesized to be less cytotoxic than non-degraded polymers. Cathepsin B is a papain-like cysteine protease with both endopeptidase and exopeptidase activity that is involved in protein degradation and turnover in cells [10]. Cathepsin B functions primarily in the endo/lysosomal compartments [27–29] and has therefore been the target for enzyme-triggered, intracellular drug delivery [30–32]. We therefore designed cationic, peptide-based polymers for nucleic acid delivery with cathepsin B linker substrates for specific endosomal degradation as a means to reduce cytotoxicity through enzyme-mediated degradation.

In this work, peptide-HPMA copolymers were synthesized via reverse addition-fragmentation chain transfer (RAFT) polymerization of HPMA with methacrylamido-peptide monomers. The peptide monomers contained an oligolysine motif that was capped with a short, four amino acid cathepsin B substrate, thereby enabling endosomal degradation of the cationic copolymers. In total, three peptide-HPMA copolymers were evaluated: (i)

pHCathK$_{10}$, containing peptides composed of the linker phe-lys-phe-leu (FKFL), a substrate of cathepsin B, connected to oligo-(L)-lysine for nucleic acid binding; (ii) pHCath(D)K$_{10}$, containing the FKFL linker with oligo-(D)-lysine; and (iii) pH(D)Cath(D)K$_{10}$, containing all (D) amino acids. These polymers were evaluated for sensitivity to cathepsin B degradation, polyplex destabilization and DNA release, cytotoxicity and transfection efficiency.

2. Materials and Methods

2.1 Materials

N-(2-hydroxypropyl)methacrylamide (HPMA) was purchased from Polysciences (Warrington, PA). The initiator VA-044 was purchased from Wako Chemicals (Richmond, VA). Fmoc-protected amino acids and HBTU were purchased from AAPPTec (Louisville, KY), N-succinimidyl methacrylate from TCI America (Portland, Oregon), and Rink Amide Resin from EMD Biosciences (Darmstad, Germany). Human liver cathepsin B was purchased from Enzo Life Sciences (Plymouth Meeting, PA). All other materials were reagent grade or better and were purchased from Sigma-Aldrich (St. Louis, MO) unless otherwise stated. Endotoxin-free plasmid pCMV-Luc2 was prepared using the Qiagen Plasmid Giga kit (Qiagen, Hilden, Germany) according to manufacturer's recommendations.

2.2 Synthesis and Enzymatic Evaluation of Peptide Monomers

2.2.1 Synthesis of Peptide Monomers—Three peptides were synthesized using (D) and (L) amino acids and 6-aminohexanoic acid (Ahx): AhxFKFLAhxK$_{10}$ (composed of only (L) amino acids); AhxFKFLAhx(D)K$_{10}$ (composed of (L) amino acid linker with oligo-(D)-lysine); and Ahx(D)FKFLAhx(D)K$_{10}$ (composed of only (D) amino acids). Peptides were synthesized on a solid support with Rink amide linker following standard Fmoc chemistry on an automated PS3 peptide synthesizer (Protein Technologies, Phoenix, AZ). Prior to peptide cleavage from the resin, the amino termini of the peptides were deprotected and coupled with N-succinimidyl methacrylate. These functionalized peptide monomers are respectively called MaAhxFKFLAhxK$_{10}$, MaAhxFKFLAhx(D)K$_{10}$, and MaAhx(D)FKFLAhx(D)K$_{10}$. Synthesized peptides were cleaved from resin by treatment of solid support with a solution of TFA/triisopropylsilane (TIPS)/1,3-dimethoxybenzene (92.5:2.5:5, v/v/v) for 2.5 hours under gentle mixing. Cleaved peptide monomers were precipitated in cold ether, dissolved in methanol and re-precipitated twice in cold ether. Each peptide monomer was analyzed by RP-HPLC and MALDI-TOF MS and shown to have greater than 95% purity after cleavage. The expected molecular weight of the peptides was 2128.82 Da. Experimentally measured molecular weights determined by MALDI-TOF MS were 2129.137 Da, 2128.526 Da, and 2128.689 Da for MaAhxFKFLAhxK$_{10}$, MaAhxFKFLAhx(d)K$_{10}$, and MaAhx(D)FKFLAhx(D)K$_{10}$, respectively.

2.2.2 Cathepsin B Cleavage of Peptide Monomers—Specific cleavage at the FKFL linker by cathepsin B was determined by adapting a method from Dubowchik *et al* [20]. For this and subsequent cathepsin B cleavage studies, human liver cathepsin B (0.351 mg/mL stock) was added to activation buffer (30 mM DTT, 15 mM EDTA) for a final concentration of 0.117 mg/mL cathepsin B, 20 mM DTT, 10 mM EDTA and incubated at 37 °C for 15 min. Reaction buffer (25 mM acetate, 1 mM EDTA, pH 5, pre-warmed at 37 °C) and peptide solution (10 mM stock) were added to the enzyme solution such that the final concentration of the reaction solution was 1.28 μg/mL cathepsin B, 24.6 mM acetate, 1.1 mM EDTA, 0.33 mM DTT, 65 μM peptide, and the reaction solution was incubated at 37 °C. Aliquots were removed at various time points and enzymatic activity stopped by addition of thioprotease inhibitor E-64 (Thermo Scientific, Waltham, MA) to a 26 μg/mL final concentration. Aliquots were analyzed qualitatively via MALDI-TOF MS.

2.2.3 Serum Stability of Peptide Macromonomers—Linker susceptibility to serum proteases was evaluated using freshly isolated mouse serum. For each peptide, peptide (5 μL of 10 mM stock) was added to serum (120 μL, pre-incubated at 37 °C). At various time points, 20 μl aliquots of the mixture were withdrawn and 5 μL of ice-cold 15% trichloroacetic acid (w/v) was added to stop enzymatic degradation via protein precipitation. Precipitated solutions were centrifuged at 13000 rpm for 15 min and supernatants were analyzed by MALDI-TOF MS.

2.3 RAFT Polymerization and Characterization of HPMA-peptide Copolymers

2.3.1. Polymer Synthesis—Three polymers were synthesized: HPMA-*co*-MaAhxFKFLAhxK$_{10}$ (pHCathK$_{10}$), HPMA-*co*-MaAhxFKFLAhx(D)K$_{10}$ (pHCath(D)K$_{10}$), and HPMA-*co*-MaAhx(D)FKFLAhx(D)K$_{10}$ (pH(D)Cath(D)K$_{10}$). Each polymer was synthesized with target degree of polymerization (DP) of 190 with 20% mole feed peptide to yield polymers with target molecular weight of approximately 103 kDa. Monomers were dissolved in acetate buffer (1 M, pH 5.1) such that the final monomer concentration of the solution was 0.7 M. The RAFT chain transfer agent (CTA) used was ethyl cyanovaleric trithiocarbonate (ECT, molecular weight 263.4 g/mol) and the initiator (I) used was VA-044. The molar ratios of total monomer:CTA:I at the start of polymerization were 190:1:0.1. The reaction solutions were transferred to round bottom flasks, capped with a rubber septum, purged with argon for 10 min, and the submerged in a 44 °C oil bath to initiate polymerization. The polymerization was allowed to proceed for 48 hrs. The flasks were removed from the oil bath and polymers dialyzed against distilled H$_2$O to removed unreacted monomers and buffer salts. The dialyzed polymers were lyophilized dry.

2.3.2. Size Exclusion Chromatography—Molecular weight analysis was carried out by size exclusion chromatography. The copolymers were dissolved at 10 mg/mL in running buffer (150 mM acetate buffer, pH 4.4) for analysis by size exclusion chromatography-multiangle light scattering (SEC-MALS). Analysis was carried out on an OHpak SB-804 HQ column (Shodex) in line with a miniDAWN TREOS multiangle light scattering detector (Wyatt, Santa Barbara, CA) and an OptiLab rEX refractive index detector (Wyatt). Absolute molecular weight averages (M_n, M_w) were calculated using ASTRA software (Wyatt).

2.3.3 Amino Acid Analysis—The actual incorporated amount of peptide and HPMA in the final copolymers was determined through modified amino acid analysis following the method of Bidlingmeyer and coworkers [33]. Briefly, hydrolyzed lysine and HPMA (which results in 1-amino-2-propanol) were derivatized with o-phthalaldehyde/β-mercaptopropionic acid and run on a Poroshell 120 EC-C18 (Agilent Technologies, Santa Clara, CA) HPLC column with pre-column derivatization to label hydrolyzed lysine and 1-amino-2-propanol. Calibration curves were generated using serial dilutions of (L)-lysine and reagent grade 1-amino-2-propanol.

2.4 Cathepsin B-mediated Polymer Degradation

Linker recognition and subsequent release of oligolysine side-chains from the polymer were assessed by enzymatic treatment with cathepsin B. For each polymer, cathepsin B reactions were set up as described previously with a final polymer concentration of 44 μg/mL. At various time points, aliquots were removed and E-64 was added to stop the enzymatic reaction. Solutions were analyzed by SEC and the relative differential refractive index profiles were compared. MALDI-TOF MS was also performed.

2.5 Polyplex Characterization and Enzymatic Susceptibility

2.5.1 Polyplex Formation—pCMV-Luc2 plasmid was diluted in ddH_2O to a concentration of 0.1 mg/mL and mixed with an equal volume of polymer (in ddH_2O water) at the desired amine to phosphate (N:P) ratio. After mixing, polyplexes were allowed for form for 10 minutes at room temperature. The charge densities of the oligolysine-*co*-HPMA copolymers, PEI, and PLL are approximately 290 mg/mmol amine, 43 mg/mmol amine, and 208 mg/mmol amine, respectively.

2.5.2 Sizing of Polyplexes by Dynamic Light Scattering (DLS)—Polyplexes (0.5 μg DNA, 10 μL) were formed with $pHCathK_{10}$, $pHCath(D)K_{10}$, $pH(D)Cath(D)K_{10}$, branched polyethylenimine (PEI, 25 kDa, PDI ~2.5) or poly-(L)-lysine (PLL, 15–30 kDa, PDI 1.2) at 3, 4, and 5 N:P ratios and were mixed with either 90 μL of ddH_2O or PBS such that the final salt concentration was 150 mM. Particle size was determined by dynamic light scattering (ZetaPLUS, Brookhaven Instruments Corp, Holtsville, NY).

2.5.3 Polyplex Destabilization by DLS—Polyplexes were formulated at 4 N:P with $pHCathK_{10}$, $pHCath(D)K_{10}$, or $pH(D)Cath(D)K_{10}$. The DLS instrument and cuvette with cap were pre-equilibrated at 37 °C. For each polyplex solution, cathepsin B reactions were set up as described previously with a final concentration of DNA of 5.33 μg/mL. Reaction solutions were transferred to the cuvette and capped to prevent evaporation. Enzymatic reaction was allowed to proceed for 8 hrs at 37 °C with particle size measured every 15 min.

2.5.4 Polyplex Unpackaging by YOYO-1 Fluorescence Quenching Assay—pCMV-Luc2 plasmid was mixed with the bis-intercalating dye YOYO-1 iodide (Invitrogen, Carlsbad, CA) at a dye/base pair ratio of 1:50 and incubated at room temperature for 1 hour. Polyplexes were formed at 4 N:P by complexing YOYO-1-labeled DNA with $pHCathK_{10}$, $pHCath(D)K_{10}$, and $pH(D)Cath(D)K_{10}$. For each polyplex solution, cathepsin B reactions were set up as described previously with a final concentration of DNA at 5.33 μg/mL. At various time points, aliquots were removed and reaction stopped with addition of E-64, diluted to 100 μL total volume with ddH_2O, and transferred to a 96-well plate. After the final time point, the fluorescence from each well of all the plates was measured on a Tecan Safire[2] plate reader (Männerdorf, Switzerland) with excitation at 491 nm and emission at 509 nm. The fluorescence signal for each time point was normalized against a plasmid-only signal.

2.6 *In vitro* Transfection Efficiency

HeLa and NIH/3T3 cells were transfected as previously described [34]. Briefly, polyplexes (1 μg DNA) were formed at 3, 4, and 5 N:P, diluted to 200 uL in MEM Reduced Serum Medium (Hyclone), and added to cells for 4 hrs. After an additional 44 hrs, luciferase expression was quantified using a luciferase assay kit (Promega, Fitchburg, WI) according to the manufacturer's instructions, except with an additional freeze-thaw cycle at −20 °C to ensure complete cell lysis. Luminescence intensity was measured on the plate reader with 1 sec integration; total protein content was measured using a BCA Protein Assay Kit (Thermo Scientific, Rockford, IL) according to the manufacturer's instructions so luciferase activity could be normalized to the total protein content. Each sample was tested in quadruplicate.

2.7 Cytotoxicity of Polymers and Polyplexes

The cytotoxicity of the polymers and polyplexes was evaluated *in vitro* using the MTS assay as described previously [34]. Polymers of various concentrations or polyplexes at 3, 4, and 5 N:P (0.2 μg DNA) were prepared in ddH_2O water and then diluted 10-fold in MEM Reduced Serum Medium. The cells were rinsed once with PBS and incubated with 40 μL of the polymer or polyplex solution for 4 hrs. At 48 hrs, 20 μL of 3-(4,5-dimethylthiazol-2-

yl)-5-(3-carboxymethoxyphenyl)-2-(4-sulfophenyl)-2*H*-tetrazolium (MTS) (Promega) was added to each well. Cells were then incubated for 3 hrs and absorbance measured at 490 nm using a plate reader. For polymers, IC_{50} values were determined using a nonlinear fit (four-parameter variable slope) in GraphPad Prism v.5 (San Diego, CA). For polyplexes, cellular viability was normalized against untreated cells.

Results

3.1 Enzymatic Degradation of Peptides by Cathepsin B and Mouse Serum

Methacrylated oligolysine (K_{10}) peptides containing the FKFL cathepsin B substrate sequence flanked on each side by a six-carbon spacer were synthesized by solid phase peptide synthesis. Three peptides were synthesized, differing only in the use of D- versus L-amino acids to impart peptidase resistance; thus, all full length peptides have MW 2128 Da. Cathepsin B-mediated peptide cleavage at the FKFL linker was monitored over 30 min enzyme incubation (Figure 1). Rapid recognition and specific cleavage of the MaAhxFKFLAhxK$_{10}$ and MaAhxFKFLAhx(D)K$_{10}$ peptides at the FKFL linker results in disappearance of the 2128 Da peak and simultaneous emergence of a 1673 Da peak corresponding to the FLAhxK$_{10}$/ FLAhx(D)K$_{10}$ fragment, respectively. Fragmentation of the original peptide is complete within 15 min of enzymatic exposure. The FLAhxK$_{10}$ peptide fragment is susceptible to exopeptidase degradation as well, with the systematic removal of C-terminal lysines over time; however, this process is considerably slower than the endopeptidase cleavage at the linker. The FLAhx(D)K$_{10}$ fragment shows resistance to exopeptidase activity. The MaAhx(D)FKFLAhx(D)K$_{10}$ peptide has no observable degradation within the 30 min of cathepsin B treatment.

Extracellular enzymatic stability of the peptide and specificity of the FKFL linker for intracellular peptidases was tested by exposing peptides to freshly isolated mouse serum and monitoring degradation over 4 hrs. No endopeptidase cleavage of the FKFL linker was detected but degradation of the MaAhxFKFLAhxK$_{10}$ peptide by non-specific exopeptidase hydrolysis was observed by 1 hr post-incubation (Figure 2a), yielding the shortened fragment MaAhxFKFLAhxK (976 Da). In contrast, intact MaAhxFKFLAhx(D)K$_{10}$ peptide is observed even after serum incubation for 4 hours. Some endopeptidase degraded product (1672 Da = FLAhx(D)K$_{10}$) is observed at the 2 and 4 hr time points (Figure 2b). No FLAhxK10 fragments are observed in 2a, likely due to rapid exopeptidase degradation by the first 30 min time point. Peaks at 656 and 1796 Da correspond to matrix and a peptide found in serum, respectively.

3.2 Enzymatic Degradation of HPMA-*co*-oligolysine Copolymers by Cathepsin B

Three HPMA-oligolysine copolymers were synthesized by RAFT polymerization of peptide monomers with HPMA as described previously [34, 35]. The synthesized polymers displayed properties close to targeted values as summarized by Table 1. In general, the copolymers had M_n ~ 5–15% lower than expected. Polydispersity of all the copolymers was below 1.2. Amino acid analysis of the copolymers revealed peptide mole incorporation around 25–27%.

Cathepsin-B mediated degradation of HPMA-oligolysine copolymers was evaluated by treating polymers with cathepsin B and analyzing polymers at various time points by size exclusion chromatography (Figure 3). Un-degraded polymers elute from the column ~13 min. Degradation of pHCathK$_{10}$ and pHCath(D)K$_{10}$ occurs within 10 min and continues up to 1 hr, as evidenced by the increased elution time of lower molecular weight polymers (Figures 3a and 3b). A secondary peak simultaneously emerges, eluting around 20 min for both copolymers. This secondary peak is attributed to released peptide after endopeptidase

cleavage of the FKFL linker ($FLAhxK_{10}$/$FLAhx(D)K_{10}$ and respective C-terminally shortened fragments). This is supported by the shifting profile of the secondary peak in the $pHCathK_{10}$ due to exopeptidase activity on the $FLAhxK_{10}$ fragment compared to a stable profile in exopeptidase-resistant $pHCath(D)K_{10}$. This is also confirmed by MALDI-TOF MS on the reaction mixture (Supplementary Information, Figure 1). $pH(D)Cath(D)K_{10}$ shows no degradation over the two hours of enzymatic treatment due to its resistance to peptidases (Figure 3c).

3.3 Polyplex Sizing and Colloidal Stability

The HPMA-oligolysine copolymers were complexed with plasmid DNA at 3, 4, and 5 N:P ratios to form nanoparticles called "polyplexes." The average hydrodynamic diameters of polyplexes in both water and 150 mM PBS were determined by dynamic light scattering. All the HPMA-oligolysine copolymers formed polyplexes with average hydrodynamic diameter of 120 nm water (Figure 4a). PEI and PLL also formed slightly smaller particles around 100 nm in diameter. In PBS, HPMA-oligolysine polyplexes remain relatively stable. The average diameter of polyplexes formed at 5 N:P increased only by 25% to 150 nm. In general, increases in size are seen with decreasing N:P ratios for all materials. In contrast, PEI and PLL particles aggregate in PBS, as indicated by the increased average diameter ranging from 500 nm to over 1 micron.

3.4 Cathepsin B-mediated Polyplex Destabilization and Unpackaging

The effects of cathepsin B exposure to $pHCathK_{10}$, $pHCath(D)K_{10}$, and $pH(D)Cath(D)K_{10}$ polyplexes were determined by monitoring particle size by DLS and DNA condensation by dye quenching assay. Polyplexes were formulated at 4 N:P and particle size measured every 15 min for 8 hrs of cathepsin B treatment (Figure 5a). Polyplexes formed with $pHCathK_{10}$ show particle size increases from ~150 nm to about 500 nm over 4hrs before plateauing. $pHCath(D)K_{10}$ shows size increases over 8 hrs up to ~600 nm in diameter. In contrast, $pH(D)Cath(D)K_{10}$ maintain particles ~150 nm in diameter with no observable size change over 8 hrs.

To monitor DNA condensation, plasmid DNA was labeled with the DNA-intercalating fluorophore YOYO-1 before complexation with polymer at 4 N:P. Plasmid condensation results in self-quenching of the YOYO-1 fluorescence due to electronic interactions between nearby YOYO-1 molecules [13]. The YOYO-1 fluorescence, normalized to that of uncomplexed plasmid, is shown in Figure 5b as a function of time of cathepsin B exposure. For the first 3 hrs, all polyplex solutions have fluorescence around 10% of free plasmid indicating efficient condensation; starting around 4 hrs, the $pHCathK_{10}$ polyplexes begin to show a trend of increasing fluorescence, up to 70% by 8 hrs. In contrast, $pHCath(D)K_{10}$ and $pH(D)Cath(D)K_{10}$ did not show any significant increase in fluorescence (unpackaging) over 8 hrs.

3.5 Plasmid DNA Delivery

Transfection efficiency of the polyplexes formed at 3, 4, and 5 N:P was tested using both HeLa and NIH/3T3 cells. The luciferase reporter transgene was used to assess gene delivery efficiency with cytotoxicity evaluated by BCA protein assay (Figure 6). In general, the HPMA-oligolysine copolymers transfected with higher efficiency than PLL over all N:P ratios. Efficiencies and trends were cell-line dependent. HeLa cells showed no significant difference in normalized transfection between the 3, 4, and 5 N:P ratios for the copolymers while PEI shows trends of increasing efficiency with increasing N:P ratio; however, copolymer materials are still within an order of magnitude less effective than PEI in transfection efficiency for N:P ratios of 4 and 5. For NIH/3T3 cells, transfection efficiencies of HPMA-oligolysine copolymers were higher with increasing N:P ratios. $pHCath(D)K_{10}$

showed the best transfection of the three copolymers, with normalized luciferase expression comparable to PEI.

3.6 Polymer Toxicity

Cytotoxicity of polymers and polyplexes was determined by MTS and BCA assay, respectively. MTS was used to determine the mitochondrial activity in HeLa and NIH/3T3 cells that had been treated with the different polymers. A range of polymer concentrations was evaluated in order to determine the IC_{50} value (concentration of polymer for 50% cell survival) for each polymer in amine equivalents. The three synthesized polymers had essentially indistinguishable IC_{50} values with overlapping confidence intervals. Determined IC_{50} values were higher in general for NIH/3T3 cells than HeLa cells and HPMA-oligolysine copolymers were less toxic than both PEI and PLL (Table 2).

The BCA assay was conducted to determine the total amount of cellular protein in lysates of transfected cells 48 hrs after transfection. Cell viability was estimated by comparing the protein levels of transfected cells with control untreated cells. Generally, a N:P of 3 was nontoxic in all polymers screened, including PLL and PEI. Toxicity increased at higher N:P ratios for the HPMA-oligolysine polymers and PLL. A trend of decreased toxicity in the $pHCathK_{10}$ polyplexes compared to $pHCath(D)K_{10}$ and $pH(D)Cath(D)K_{10}$ polyplexes for all N:P ratios in both cell types was observed ($p < 0.01$). This trend is confirmed in HeLa cells treated with polyplexes via the MTS assay (Figure 7).

4. Discussion

In previous work, we reported the synthesis of pendant peptide copolymers with HPMA synthesized by living polymerization and their application for nucleic acid delivery [34, 35]. RAFT polymerization of this class of materials resulted in better controlled peptide incorporation, lower polydispersity and decreased cytotoxicity compared to similar polymers prepared by free radical polymerization [19, 36]. In previous work, we found optimal polymers contained 20 mole percent K_{10} with transfection efficiency of these polymers in cultured cells similar to that of branched PEI [34]. The goal of this work is to develop peptide-HPMA materials that undergo triggered endosomal-degradation and cargo release in response to specific enzymatic activity. Our strategy is to include an enzymatically cleavable linker between the peptide and the polymer HPMA backbone. Because peptide content in these polymers is high, complete cleavage would result in a 60% reduction in polymer molecular weight and the release of short oligolysine peptides from an HPMA-based polymer backbone.

Cathepsin B was selected as the targeted enzyme for its endo-lysosomal activity. With a papain-like structure, cathepsin B has two domains with the active site cleft along the interface [37]. The peptidyl substrate amino acids are conventionally named … P2-P1-P1'-P2'…, where the peptide bond is cleaved between P1 and P1' [38]. In this study, the sequence FKFL, where F=P2, K=P1, F=P1' and L=P2', was used as the cathepsin B substrate linkage. Several studies have systematically evaluated various amino acids to optimize the substrate sequence for cathepsin B. These studies show that a phenylalanine in P2 gives the highest cathepsin B hydrolysis rate (k_{cat}/K_m) [39–41]. Arginine is the most preferred amino acid for the P1 position, although a lysine in this position is also accepted with about 50% relative activity compared to arginine [39, 40]. Dubowchik and Firestone utilized a lysine at P1 in their immunoconjugate BR96-Dox because of potential improved systemic stability compared to arginine [20, 42]. Based on this rationale, a lysine at P1 was also used for this work. Initially a peptide was designed with lysines in the P1' and P2' positions (peptide $MaAhxFK_{10}$) but no specific endopeptidase cleavage was observed with this substrate (data not shown). Because of reports showing that hydrophobic amino acids

are preferred in both the P1' and P2' positions, the amino acids F and L were used, respectively. Phenylalanine was used at the P1' position due to reports showing optimal cathepsin B cleavage in sequences with this amino acid at P1' [40, 43]. Finally, a six carbon linker (6-aminohexanoic acid) was included flanking both sides of the FKFL to provide spacers for the cathepsin substrate sequence both from the polymer backbone and the cationic K_{10} nucleic acid binding domain in attempt to provide better access to cathepsin B. The resulting peptide, MaAhxFKFLAhxK_{10}, was shown to be recognized by cathepsin B and cleaved within 15 min (Figure 1).

Cathepsin B exhibits both specific endopeptidase and exopeptidase activity, with the former dominating at pH 6–7 and the latter optimal at pH < 5.0 [44]. Three peptides were therefore synthesized: MaAhxFKFLAhxK_{10}, which is susceptible to both endopeptidase and exopeptidase activity; MaAhxFKFLAhx(D)K_{10}, which is susceptible only to endopeptidase activity; and MaAhx(D)FKFLAhx(D)K_{10}, which is protease resistant. Sensitivity of these peptides to cathepsin B-mediated proteolysis was evaluated at pH 5.0. This pH was selected because it is representative of the late endosome milieu where both endopeptidase and exopeptidase activity would be expected [45]. At this pH, the endopeptidase activity is about 15% of optimum activity at pH ~6.2 while exopeptidase activity is about 80% of optimal activity. Degradation of the three peptides by cathepsin B followed expected patt erns with faster kinetics for endopeptidase activity compared to exopeptidase activity (Figure 1).

Ideally, the peptide-based polymers would remain stable during circulation to protect nucleic acids from serum nucleases. In addition to nucleases, serum contains many peptidases, such as dipeptidyl peptidases and endopeptidases [46–49]. To assess serum stability, peptides were incubated with freshly isolated mouse serum (Figure 2). Degradation of MaAhxFKFLAhxK_{10} was complete by 1 hr, resulting in the shortened MaAhxFKFLAhxK fragment. In contrast, full length MaAhxFKFLAhx(D)K_{10} is detected even after a 4 hr serum incubation, although some endopeptidase degraded product (1672 Da = FLAhx(D)K_{10}) is observed after 1 hr. It should be noted that in the presence of cathepsin B, endopeptidase degradation of this peptide is observed within 5 min. The analogous FLAhxK_{10} fragment from MaAhxFKFLAhxK_{10} likely is rapidly degraded by carboxypeptidases and thus is not detected on MALDI. The MaAhxFKFLAhx(D)K_{10} peptide is a promising building block for polymers used in *in vivo* applications requiring specific intracellular degradation. While stability in murine serum may not correlate to human serum, high homology in the degradomes (> 80% strict orthologues) between mice and humans suggests information regarding enzymatic substrate specificity may be gained from these serum studies [50].

Copolymerization of the methacrylated peptides with HPMA by RAFT polymerization yielded polymers with narrow polydispersity, expected composition, and near-target molecular weights (Table 1). Cathepsin B-mediated degradation of polymers was evaluated at pH 5.0 by size exclusion chromatography (Figure 3). Accessibility of cathepsin B to linker sites incorporated in dendrimers has been shown to be restricted due to steric hindrance for some systems [51]. However, synthesized pHCathK_{10} and pHCath(D)K_{10} polymers susceptible to cathepsin B cleavage show rapid reduction in size within 10 min and complete cleavage of oligolysine side chains from the polymer backbone within one hour, leading to a theoretical reduction of ~60% in molecular weight. The kinetics of proteolysis for the peptide and polymers are similar as seen by comparing peptide monomer (Figure 1) and copolymer (Supplementary Figure 1) fragmentation. In comparison, pH(D)Cath(D)K_{10} shows complete enzymatic resistance. HPMA-*co*-MaAhxK_{10} copolymers were also treated with cathepsin B and the observed MW shift over 4hrs is comparable to 10 min with pHCathK_{10} (data not shown). In addition to rapid copolymer size reduction, labile side-chains can potentially increase accessibility of peptide side-chains for other peptidases;

this is observed in the peptide peak (~20 min) released by degradation of pHCathK$_{10}$ but not pHCath(D)K$_{10}$ (Figures 3a and 3b).

All polymers efficiently complexed DNA and formed polyplexes with diameters ~100–200 nm that are stable in physiological salt concentrations (Figure 4). While poly-(L)-lysine-based polyplexes are not stable in 150 mM PBS, inclusion of HPMA in the backbone of the cationic polymer prevents salt-induced aggregation [34, 36, 52]. Controlled polyplex unpackaging and DNA release after cellular internalization is integral to efficient gene delivery and expression [10]. Effective delivery requires extracellular and endosomal stability with cytosolic unpackaging for eventual expression. Cathepsin B-mediated unpackaging of polyplexes formed from pHCathK$_{10}$, pHCath(D)K$_{10}$ and pH(D)Cath(D)K$_{10}$ was studied by dynamic light scattering and YOYO-1 fluorescence quenching assay. pHCathK$_{10}$ and pHCath(D)K$_{10}$ polyplexes both show increasing particle size over time while pH(D)Cath(D)K$_{10}$ particles remain unchanged, suggesting enzymatically-driven polyplex destabilization. DNA packaging was also assessed through YOYO-1 fluorescence quenching assay, which monitors DNA decondensation as YOYO-1 fluorescence is restored when these molecules are not in close proximity to each other. Decondensation of DNA from polyplexes is only observed with pHCathK$_{10}$ and not pHCath(D)K$_{10}$ or pHK10 (data not shown). Oligolysines as short as 8-mers are able to condense DNA [24, 53], so despite cleavage of oligolysine side chains from the HPMA backbone, oligolysine fragments may remain able to form relatively large and unstable, but intact, polyplexes. Since oligo-(D)-lysine is resistant to further degradation, it will remain bound to DNA thereby keeping it packaged; in contrast, oligo-(L)-lysine, subject to exopeptidase degradation, will eventually release DNA upon further degradation. This is supported by the observation that YOYO-1 fluorescence from polyplexes formed by oligo-(L)-lysine increases with time when incubated with cathepsin B but polyplexes formed by oligo-(D)-lysine do not (data not shown).

While reducible HPMA-oligolysine copolymers have significantly lower transfection efficiency compared to their non-degradable counterparts [19], the enzymatically-cleavable polymers described here (pHCathK$_{10}$ and pHCath(D)K$_{10}$) have similar transfection efficiencies to non-degradable pH(D)Cath(D)K$_{10}$ in cultured cells (Figures 6a and 6b). Endosomal/lysosomal unpackaging may not increase transfection without compartmental escape for cytosolic release. Transfection was also evaluated in serum conditions (data not shown). Reduced transfection efficiency compared to serum-free transfections was observed, as reported previously for similar polymers [19]. No significant difference in transfection efficiency was noted between the three polymers even in serum conditions (data not shown), possibly because of altered protease activities in heat-inactivated serum. Cationic polymers have been implicated in toxicity through both necrotic and apoptotic routes [12, 26, 54, 55]. Electrostatic interactions with the plasma membrane cause permeabilization and pore formation, triggering cellular efflux of cytosolic contents and necrosis [54]. Compromised mitochondrial and lysosomal membranes lead to release of pro-apoptotic factors cytochrome c and cathepsins, respectively, initiating apoptotic cascades [56, 57]. Degradation of cationic polymers prior to cytosolic release or endo-lysosomal fusion can potentially decrease induction of apoptosis and reduce cytotoxicity. The relative toxicity pHCathK$_{10}$, pHCath(D)K$_{10}$ and pH(D)Cath(D)K$_{10}$ was evaluated in HeLa and NIH/3T3 cells using the MTS assay (Table 2). Results suggest similar toxicity between the three synthesized polymers regardless of enzymatic susceptibility. One possible explanation is that for free polymer the primary route of toxicity might be through plasma membrane disruption and permeabilization as implicated for PEI [12]. Therefore, intracellularly-controlled degradation will not significantly affect toxicity. This hypothesis is supported by the observation that polyplexes formed with pHCathK$_{10}$ are less toxic than pHCath(D)K$_{10}$ and pH(D)Cath(D)K$_{10}$ polyplexes at all tested charge ratios and in both HeLa and NIH/3T3 cells (Figures 6c and 6d, Figure 7). This result was confirmed both by protein content

analysis and MTS assay of cells exposed to polyplexes. In the polyplex form, a reduced amount of free polymer is available to disrupt the cellular membrane and the effect of intracellular degradation on cytotoxicity may be more pronounced. $pHCathK_{10}$ can be degraded additionally by exopeptidases, allowing for accelerated degradation and reduced toxicity compared to $pHCath(D)K_{10}$. Still, substantial toxicity is still observed with the $pHCathK_{10}$ polyplexes formed at higher N:P ratios. One potential approach that may further reduce toxicity of future generations of these polymers is to decrease the cationic charge density by including non-charged amino acids in the nucleic acid binding sequence. High charge density has been correlated with cytotoxicity for several cationic polymers [12, 58, 59].

Conclusions

In summary, peptide-based polycations that are susceptible to cathepsin B-catalyzed degradation were synthesized. The polymers were shown to undergo rapid degradation in the presence of cathepsin B. When packaged into nanoparticles by complexation with nucleic acids, linkers remain sufficiently available to fit into catalytic pockets of endopeptidases and be specifically degraded. Thus, we have demonstrated triggered nanoparticle degradation by a selective enzymatic mechanism.

Supplementary Material

Refer to Web version on PubMed Central for supplementary material.

Acknowledgments

References

[1]. Pack DW, Hoffman AS, Pun S, Stayton PS. Design and development of polymers for gene delivery. Nat. Rev. Drug Discov. 2005; 4:581–593. [PubMed: 16052241]

[2]. Chollet P, Favrot MC, Hurbin A, Coll JL. Side-effects of a systemic injection of linear polyethylenimine-DNA complexes. J. Gene Med. 2002; 4:84–91. [PubMed: 11828391]

[3]. Ward CM, Read ML, Seymour LW. Systemic circulation of poly(L-lysine)/DNA vectors is influenced by polycation molecular weight and type of DNA: differential circulation in mice and rats and the implications for human gene therapy. Blood. 2001; 97:2221–2229. [PubMed: 11290582]

[4]. Burke RS, Pun SH. Extracellular barriers to in vivo PEI and PEGylated PEI polyplex-mediated gene delivery to the liver. Bioconjug. Chem. 2008; 19:693–704. [PubMed: 18293906]

[5]. Grigsby CL, Leong KW. Balancing protection and release of DNA: tools to address a bottleneck of nonviral gene delivery. J. R. Soc. Interface. 2010; 7(Suppl 1):S67–82. [PubMed: 19734186]

[6]. Luten J, van Nostrum CF, De Smedt SC, Hennink WE. Biodegradable polymers as non-viral carriers for plasmid DNA delivery. J. Control. Release. 2008; 126:97–110. [PubMed: 18201788]

[7]. Fischer D, Osburg B, Petersen H, Kissel T, Bickel U. Effect of poly(ethylene imine) molecular weight and pegylation on organ distribution and pharmacokinetics of polyplexes with oligodeoxynucleotides in mice. Drug Metab. Dispos. 2004; 32:983–992. [PubMed: 15319340]

[8]. Mullen PM, Lollo CP, Phan QC, Amini A, Banaszczyk MG, Fabrycki JM, Wu D, Carlo AT, Pezzoli P, Coffin CC, Carlo DJ. Strength of conjugate binding to plasmid DNA affects degradation rate and expression level in vivo. Biochim. Biophys. Acta. 2000; 1523:103–110. [PubMed: 11099863]

[9]. Nishikawa M, Takemura S, Takakura Y, Hashida M. Targeted delivery of plasmid DNA to hepatocytes in vivo: optimization of the pharmacokinetics of plasmid DNA/galactosylated poly(L-lysine) complexes by controlling their physicochemical properties. J. Pharmacol. Exp. Ther. 1998; 287:408–415. [PubMed: 9765363]

[10]. Schaffer DV, Fidelman NA, Dan N, Lauffenburger DA. Vector unpacking as a potential barrier for receptor-mediated polyplex gene delivery. Biotechnol. Bioeng. 2000; 67:598–606. [PubMed: 10649234]

[11]. de Wolf HK, de Raad M, Snel C, van Steenbergen MJ, Fens MHAM, Storm G, Hennink WE. Biodegradable poly(2-dimethylamino ethylamino)phosphazene for in vivo gene delivery to tumor cells. Effect of polymer molecular weight. Pharm. Res. 2007; 24:1572–1580. [PubMed: 17435970]

[12]. Fischer D, Li Y, Ahlemeyer B, Krieglstein J, Kissel T. In vitro cytotoxicity testing of polycations: influence of polymer structure on cell viability and hemolysis. Biomaterials. 2003; 24:1121–1131. [PubMed: 12527253]

[13]. Breunig M, Lungwitz U, Liebl R, Goepferich A. Breaking up the correlation between efficacy and toxicity for nonviral gene delivery. P. Natl. Acad. Sci. USA. 2007; 104:14454–14459.

[14]. Mintzer MA, Simanek EE. Nonviral Vectors for Gene Delivery. Chem. Rev. 2009; 109:259–302. [PubMed: 19053809]

[15]. Meng FH, Hennink WE, Zhong Z. Reduction-sensitive polymers and bioconjugates for biomedical applications. Biomaterials. 2009; 30:2180–2198. [PubMed: 19200596]

[16]. Lynn DM, Langer R. Degradable poly(beta-amino esters): Synthesis, characterization, and self-assembly with plasmid DNA. J. Am. Chem. Soc. 2000; 122:10761–10768.

[17]. Meister A, Anderson ME. Glutathione. Annu. Rev. Biochem. 1983; 52:711–760. [PubMed: 6137189]

[18]. Sun WC, Davis PB. Reducible DNA nanoparticles enhance in vitro gene transfer via an extracellular mechanism. J. Control. Release. 2010; 146:118–127. [PubMed: 20438780]

[19]. Shi J, Johnson RN, Schellinger JG, Carlson PM, Pun SH. Reducible HPMA-co-oligolysine copolymers for nucleic acid delivery. Int. J. Pharm. 2011

[20]. Dubowchik GM, Firestone RA, Padilla L, Willner D, Hofstead SJ, Mosure K, Knipe JO, Lasch SJ, Trail PA. Cathepsin B-labile dipeptide linkers for lysosomal release of doxorubicin from internalizing immunoconjugates: model studies of enzymatic drug release and antigen-specific in vitro anticancer activity. Bioconjug. Chem. 2002; 13:855–869. [PubMed: 12121142]

[21]. Hortin GL, Warshawsky I, Laude-Sharp M. Macromolecular chromogenic substrates for measuring proteinase activity. Clin. Chem. 2001; 47:215–222. [PubMed: 11159769]

[22]. Doronina SO, Toki BE, Torgov MY, Mendelsohn BA, Cerveny CG, Chace DF, DeBlanc RL, Gearing RP, Bovee TD, Siegall CB, Francisco JA, Wahl AF, Meyer DL, Senter PD. Development of potent monoclonal antibody auristatin conjugates for cancer therapy. Nat. Biotechnol. 2003; 21:778–784. [PubMed: 12778055]

[23]. Levesque SG, Shoichet MS. Synthesis of enzyme-degradable, peptide-cross-linked dextran hydrogels. Bioconjug. Chem. 2007; 18:874–885. [PubMed: 17402704]

[24]. Wang Y, Mangipudi SS, Canine BF, Hatefi A. A designer biomimetic vector with a chimeric architecture for targeted gene transfer. J. Control. Release. 2009; 137:46–53. [PubMed: 19303038]

[25]. Grosse SM, Tagalakis AD, Mustapa MF, Elbs M, Meng QH, Mohammadi A, Tabor AB, Hailes HC, Hart SL. Tumor-specific gene transfer with receptor-mediated nanocomplexes modified by polyethylene glycol shielding and endosomally cleavable lipid and peptide linkers. FASEB J. 2010; 24:2301–2313. [PubMed: 20203088]

[26]. Hunter AC, Moghimi SM. Cationic carriers of genetic material and cell death: a mitochondrial tale. Biochim. Biophys. Acta. 2010; 1797:1203–1209. [PubMed: 20381448]

[27]. Authier F, Metioui M, Bell AW, Mort JS. Negative regulation of epidermal growth factor signaling by selective proteolytic mechanisms in the endosome mediated by cathepsin B. J. Biol. Chem. 1999; 274:33723–33731. [PubMed: 10559264]

[28]. Blum JS, Fiani ML, Stahl PD. Proteolytic cleavage of ricin A chain in endosomal vesicles. Evidence for the action of endosomal proteases at both neutral and acidic pH. J. Biol. Chem. 1991; 266:22091–22095. [PubMed: 1939230]

[29]. Lautwein A, Kraus M, Reich M, Burster T, Brandenburg J, Overkleeft HS, Schwarz G, Kammer W, Weber E, Kalbacher H, Nordheim A, Driessen C. Human B lymphoblastoid cells contain distinct patterns of cathepsin activity in endocytic compartments and regulate MHC class II transport in a cathepsin S-independent manner. J. Leukoc. Biol. 2004; 75:844–855. [PubMed: 14966190]

[30]. Kopecek J, Kopeckova P, Minko T, Lu Z. HPMA copolymer-anticancer drug conjugates: design, activity, and mechanism of action. Eur. J. Pharm. Biopharm. 2000; 50:61–81. [PubMed: 10840193]

[31]. Sutherland MS, Sanderson RJ, Gordon KA, Andreyka J, Cerveny CG, Yu C, Lewis TS, Meyer DL, Zabinski RF, Doronina SO, Senter PD, Law CL, Wahl AF. Lysosomal trafficking and cysteine protease metabolism confer target-specific cytotoxicity by peptide-linked anti-CD30-auristatin conjugates. J. Biol. Chem. 2006; 281:10540–10547. [PubMed: 16484228]

[32]. Ulbrich K, Subr V, Strohalm J, Plocova D, Jelinkova M, Rihova B. Polymeric drugs based on conjugates of synthetic and natural macromolecules. I. Synthesis and physico-chemical characterisation. J. Control. Release. 2000; 64:63–79. [PubMed: 10640646]

[33]. Bidlingmeyer BA, Cohen SA, Tarvin TL. Rapid analysis of amino acids using pre-column derivatization. J. Chromatogr. 1984; 336:93–104. [PubMed: 6396315]

[34]. Johnson RN, Chu DS, Shi J, Schellinger JG, Carlson PM, Pun SH. HPMA-oligolysine copolymers for gene delivery: Optimization of peptide length and polymer molecular weight. J. Control. Release. 2011

[35]. Johnson RN, Burke RS, Convertine AJ, Hoffman AS, Stayton PS, Pun SH. Synthesis of Statistical Copolymers Containing Multiple Functional Peptides for Nucleic Acid Delivery. Biomacromolecules. 2010

[36]. Burke RS, Pun SH. Synthesis and characterization of biodegradable HPMA-oligolysine copolymers for improved gene delivery. Bioconjug. Chem. 2010; 21:140–150. [PubMed: 19968270]

[37]. Guha S, Padh H. Cathepsins: fundamental effectors of endolysosomal proteolysis. Indian J. Biochem. Biophys. 2008; 45:75–90. [PubMed: 21086720]

[38]. Schechter I, Berger A. On the size of the active site in proteases. I. Papain. Biochem. Biophys. Res. Commun. 1967; 27:157–162. [PubMed: 6035483]

[39]. Cezari MH, Puzer L, Juliano MA, Carmona AK, Juliano L. Cathepsin B carboxydipeptidase specificity analysis using internally quenched fluorescent peptides. Biochem. J. 2002; 368:365–369. [PubMed: 12201820]

[40]. Cotrin SS, Puzer L, de Souza Judice WA, Juliano L, Carmona AK, Juliano MA. Positional-scanning combinatorial libraries of fluorescence resonance energy transfer peptides to define substrate specificity of carboxydipeptidases: assays with human cathepsin B. Anal. Biochem. 2004; 335:244–252. [PubMed: 15556563]

[41]. Hasnain S, Hirama T, Tam A, Mort JS. Characterization of recombinant rat cathepsin B and nonglycosylated mutants expressed in yeast. New insights into the pH dependence of cathepsin B-catalyzed hydrolyses. J. Biol. Chem. 1992; 267:4713–4721. [PubMed: 1537854]

[42]. Dubowchik GM, Firestone RA. Cathepsin B-sensitive dipeptide prodrugs. 1. A model study of structural requirements for efficient release of doxorubicin. Bioorg. Med. Chem. Lett. 1998; 8:3341–3346. [PubMed: 9873731]

[43]. Stachowiak K, Tokmina M, Karpinska A, Sosnowska R, Wiczk W. Fluorogenic peptide substrates for carboxydipeptidase activity of cathepsin B. Acta Biochim. Pol. 2004; 51:81–92. [PubMed: 15094828]

[44]. Polgar L, Csoma C. Dissociation of ionizing groups in the binding cleft inversely controls the endo- and exopeptidase activities of cathepsin B. J. Biol. Chem. 1987; 262:14448–14453. [PubMed: 3312190]

[45]. Killisch I, Steinlein P, Romisch K, Hollinshead R, Beug H, Griffiths G. Characterization of early and late endocytic compartments of the transferrin cycle. Transferrin receptor antibody blocks

erythroid differentiation by trapping the receptor in the early endosome. J. Cell Sci. 1992; 103(Pt 1):211–232. [PubMed: 1429906]

[46]. Durinx C, Lambeir AM, Bosmans E, Falmagne JB, Berghmans R, Haemers A, Scharpe S, De Meester I. Molecular characterization of dipeptidyl peptidase activity in serum: soluble CD26/ dipeptidyl peptidase IV is responsible for the release of X-Pro dipeptides. Eur. J. Biochem. 2000; 267:5608–5613. [PubMed: 10951221]

[47]. Erdos EG, Skidgel RA. Neutral endopeptidase 24.11 (enkephalinase) and related regulators of peptide hormones. FASEB J. 1989; 3:145–151. [PubMed: 2521610]

[48]. Mentlein R, Gallwitz B, Schmidt WE. Dipeptidyl-peptidase IV hydrolyses gastric inhibitory polypeptide, glucagon-like peptide-1(7–36)amide, peptide histidine methionine and is responsible for their degradation in human serum. Eur. J. Biochem. 1993; 214:829–835. [PubMed: 8100523]

[49]. Wang LH, Ahmad S, Benter IF, Chow A, Mizutani S, Ward PE. Differential processing of substance P and neurokinin A by plasma dipeptidyl(amino)peptidase IV, aminopeptidase M and angiotensin converting enzyme. Peptides. 1991; 12:1357–1364. [PubMed: 1726123]

[50]. Puente XS, Sanchez LM, Overall CM, Lopez-Otin C. Human and mouse proteases: a comparative genomic approach. Nat. Rev. Genet. 2003; 4:544–558. [PubMed: 12838346]

[51]. Etrych T, Strohalm J, Chytil P, Cernoch P, Starovoytova L, Pechar M, Ulbrich K. Biodegradable star HPMA polymer conjugates of doxorubicin for passive tumor targeting. Eur. J. Pharm. Sci. 2011; 42:527–539. [PubMed: 21392579]

[52]. Kasuya Y, Lu ZR, Kopeckova P, Minko T, Tabibi SE, Kopecek J. Synthesis and characterization of HPMA copolymer-aminopropylgeldanamycin conjugates. J. Control. Release. 2001; 74:203–211. [PubMed: 11489496]

[53]. Mann A, Thakur G, Shukla V, Ganguli M. Peptides in DNA delivery: current insights and future directions. Drug Discov. Today. 2008; 13:152–160. [PubMed: 18275913]

[54]. Hong S, Leroueil PR, Janus EK, Peters JL, Kober MM, Islam MT, Orr BG, Baker JR Jr. Banaszak Holl MM. Interaction of polycationic polymers with supported lipid bilayers and cells: nanoscale hole formation and enhanced membrane permeability. Bioconjug. Chem. 2006; 17:728–734. [PubMed: 16704211]

[55]. Moghimi SM, Symonds P, Murray JC, Hunter AC, Debska G, Szewczyk A. A two-stage poly(ethylenimine)-mediated cytotoxicity: implications for gene transfer/therapy. Molecular Therapy. 2005; 11:990–995. [PubMed: 15922971]

[56]. Klemm AR, Young D, Lloyd JB. Effects of polyethyleneimine on endocytosis and lysosome stability. Biochem. Pharmacol. 1998; 56:41–46. [PubMed: 9698087]

[57]. Droga-Mazovec G, Bojic L, Petelin A, Ivanova S, Romih R, Repnik U, Salvesen GS, Stoka V, Turk V, Turk B. Cysteine cathepsins trigger caspase-dependent cell death through cleavage of bid and antiapoptotic Bcl-2 homologues. J. Biol. Chem. 2008; 283:19140–19150. [PubMed: 18469004]

[58]. Allen MH, Green MD, Getaneh HK, Miller KM, Long TE. Tailoring charge density and hydrogen bonding of imidazolium copolymers for efficient gene delivery. Biomacromolecules. 2011; 12:2243–2250. [PubMed: 21557603]

[59]. Hwang SJ, Bellocq NC, Davis ME. Effects of structure of beta-cyclodextrin-containing polymers on gene delivery. Bioconjug. Chem. 2001; 12:280–290. [PubMed: 11312690]
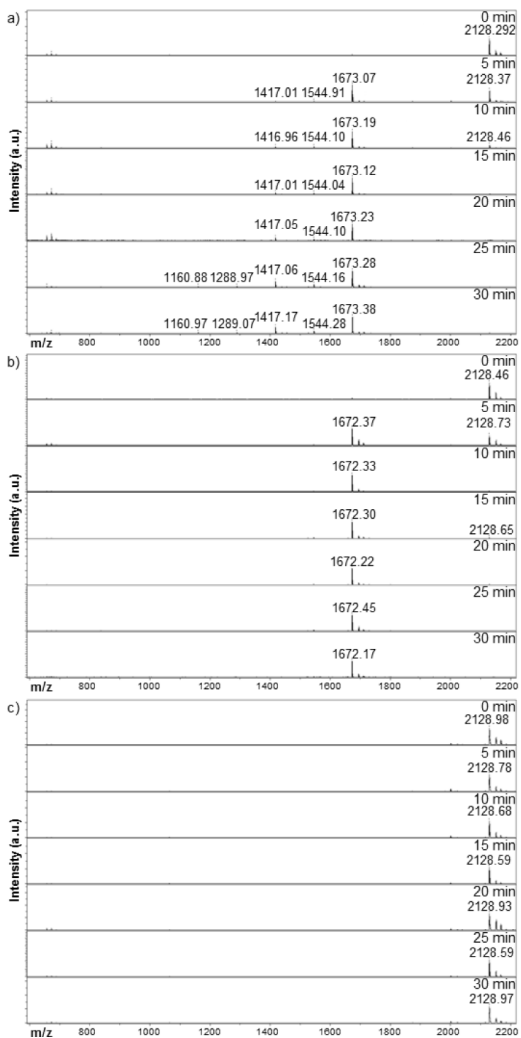
Figure 1.
MALDI-TOF MS time-point study of cathepsin B-mediated fragmentation of (a)
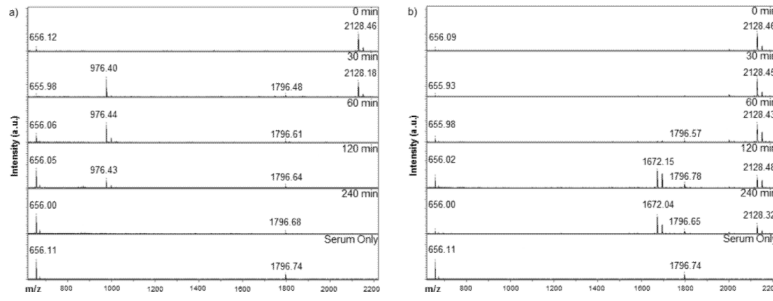MaAhxFKFLAhxK$_{10}$, (b) MaAhxFKFLAhx(D)K)$_{10}$, and (c) MaAhx(D)FKFLAhx(DK$_{10}$

Figure 2.
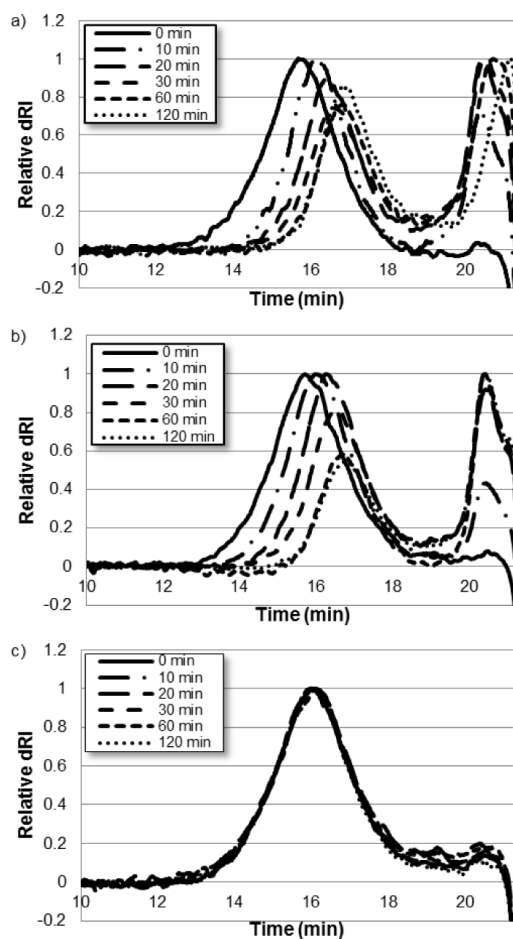MALDI-TOF MS time-point study of mouse serum enzymatic digest of (a) MaAhxFKFLAhxK$_{10}$, (b) MaAhxFKFLAhx($_D$)K$_{10}$

Figure 3.
Overlaid size exclusion chromatography of cathepsin B degradation of (a) pHCathK$_{10}$, (b) pHCath(D)K$_{10}$, and (c) pH(D)Cath(D)K$_{10}$.
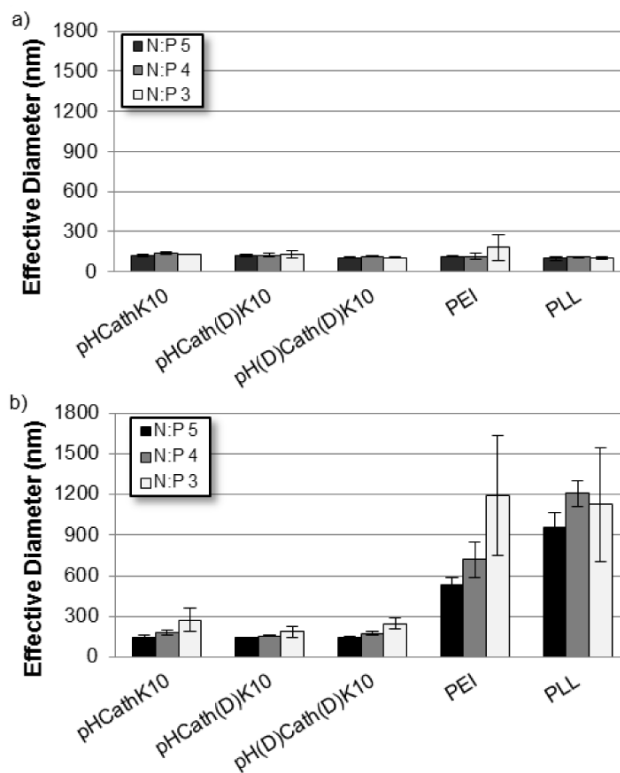
Figure 4.
DLS sizing of polyplexes in (a) ddH$_2$O and (b) 150mM PBS
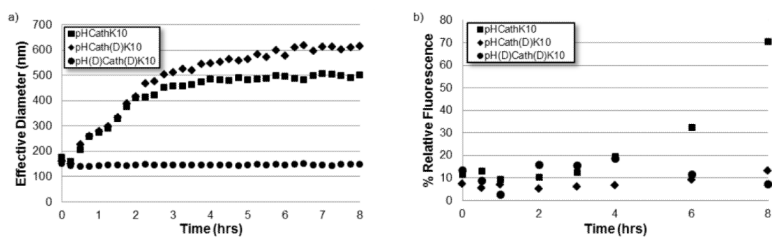
Figure 5.
Polyplex destabilization and unpackaging of pHCathK$_{10}$/DNA, pHCath($_D$)K$_{10}$/DNA, and pH($_D$)Cath($_D$)K$_{10}$/DNA polyplexes as measured by (a) dynamic light scattering and (b) YOYO-1 fluorescence quenching assay.
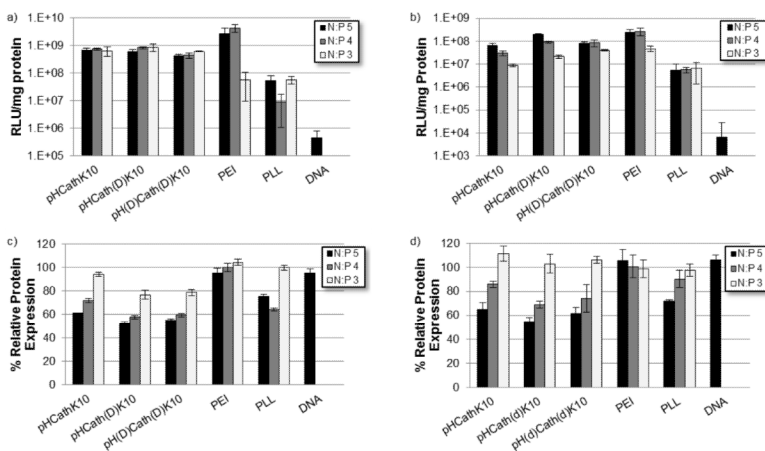
Figure 6.
Normalized luminescence per mg protein as a measure for transfection efficiency in (a) HeLa and (b) NIH/3T3 cells. Protein expression normalized to untreated cells for (c) HeLa and (d) NIH/3T3 cells.
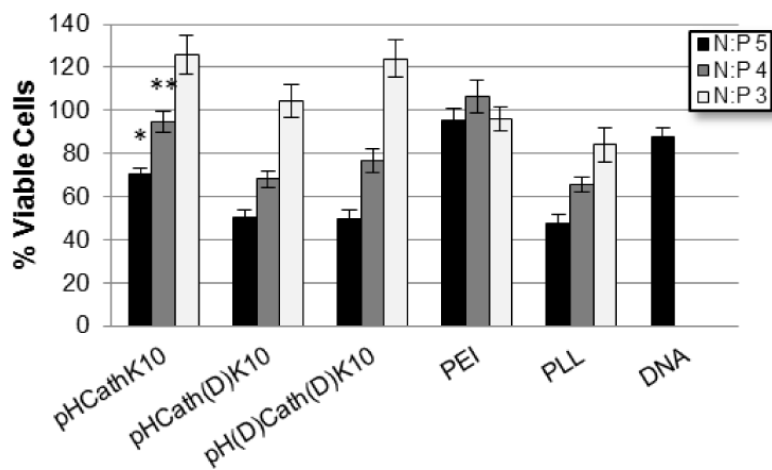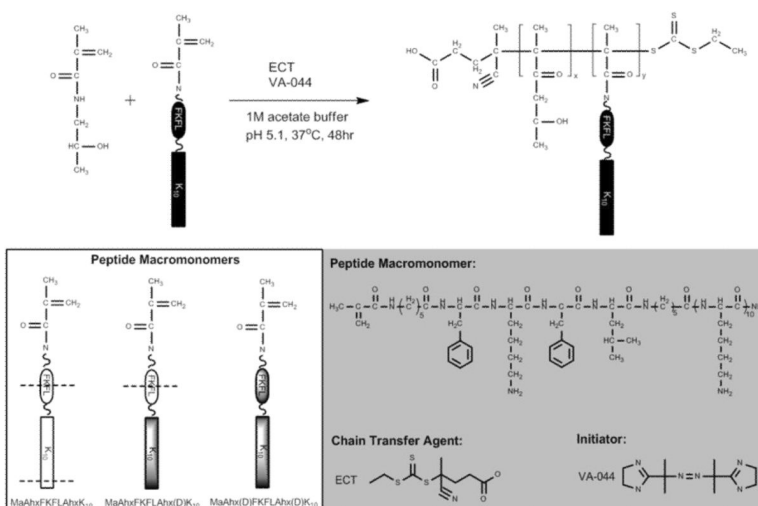
Figure 7.
Cellular viability of HeLa cells treated with polyplexes measured via MTS assay.
pHCathK$_{10}$ are significantly less toxic than pHCath(D)K$_{10}$, pH(D)Cath(D)K$_{10}$, and PLL at
*N:P 5 and **N:P 4 (p < 0.01).

Scheme 1.
Synthetic scheme of HPMA-*co*-oligolysine copolymers

Table 1

Properties of HPMA–oligolysine copolymers

HPMA-oligolysine Copolymer	Peptide Monomer	Degradation Type	Targeted M_n (kDa)[a]	Determined M_n (kDa)[b]	M_w/M_n[b]	Mole% Peptide Monomer[c]
pHCathK$_{10}$	MaAhxFKPLAhxK$_{10}$	Endo/exopeptidase	102.63	96.64	1.17	27.4
pHCath(D)K$_{10}$	MaAhxFKPLAhx(D)K$_{10}$	Exopeptidase only	102.63	93.26	1.17	24.8
pH(D)Cath(D)K$_{10}$	MaAhx(D)FKFLAhx(D)K$_{10}$	None	102.63	88.57	1.18	26.0

[a] Based on Mn=[Mo]/[CTAo] × conversion × FW with no counterions.

[b] Determined by SEC-MALS.

[c] Determined by amino acid analysis.

Table 2

Polymer Toxicity

Polymer	HeLa		NIH/3T3	
	IC_{50} (μg/mL)	IC_{50} (μM 1° N)	IC_{50} (μg/mL)	IC_{50} (μM 1° N)
pHCathK$_{10}$	16.2	53	29.7	97.3
pHCath(D)K$_{10}$	16.3	53.5	28.7	94
pH(D)Cath(D)K$_{10}$	14.3	46.7	30.3	99.3
PEI	4.5	26.4	8.3	48.3
PLL	7.2	34.4	17.9	86.1